HAL open science

Ternary switchable phase transition of CaCO3 by shock waves

A. Sivakumar, P. Shailaja, M. Nandhini, S.S. Jude Dhas, R.S. Kumar, A.I. Almansour, N. Arumugam, Shubhadip Chakraborty, S.A.M. Britto Dhas

To cite this version:

A. Sivakumar, P. Shailaja, M. Nandhini, S.S. Jude Dhas, R.S. Kumar, et al.. Ternary switchable phase transition of CaCO3 by shock waves. Ceramics International, 2022, 48 (6), pp.8457-8465. 10.1016/j.ceramint.2021.12.055 . hal-03596294

HAL Id: hal-03596294

https://hal.science/hal-03596294v1

Submitted on 30 Mar 2022

HAL is a multi-disciplinary open access archive for the deposit and dissemination of scientific research documents, whether they are published or not. The documents may come from teaching and research institutions in France or abroad, or from public or private research centers.

L'archive ouverte pluridisciplinaire **HAL**, est destinée au dépôt et à la diffusion de documents scientifiques de niveau recherche, publiés ou non, émanant des établissements d'enseignement et de recherche français ou étrangers, des laboratoires publics ou privés.

Distributed under a Creative Commons Attribution - NonCommercial 4.0 International License

Journal Pre-proof

Ternary Switchable Phase Transition of $CaCO_3$ by Shock Waves

A.Sivakumar[1], P.Shailaja[1], M.Nandhini[1], S.Sahaya Jude Dhas[2], Raju Suresh Kumar[3], Abdulrahman I. Almansour[3], , Natarajan Arumugam[3], Shubhadip Chakraborty[4], S.A.Martin Britto Dhas[1]*

[1]Department of Physics, Abdul Kalam Research Center, Sacred Heart College, Tirupattur, Vellore, Tamil Nadu, India – 635 601

[2]Department of Physics, Kings Engineering College, Sriperumbudur, Chennai, Tamilnadu, India - 602 117

[3]Department of Chemistry, College of Science, King Saud University, P.O. Box 2455, Riyadh, Saudi Arabia- 11451

[4]Institut de Physique de Rennes, UMR CNRS 6251, Université de Rennes 1, 35042 Rennes Cedex, France

Corresponding Author: martinbritto@shctpt.edu

Abstract

In the present article, we disclose shock wave induced crystallographic switchable phase transition of calcium carbonate nano particles ($CaCO_3$ NPs). The observed profiles of powder X-ray diffraction reveal that $CaCO_3$ NPs undergoes phase transitions in the sequential order from Calcite-I to Calcite-II and Calcite-II to Calcite-III at 50 and 100 shocks, respectively. Interestingly, reversible phase transitions have been observed from Calcite-III to Calcite-II and Calcite-II to Calcite-I at 150 and 200 shocked conditions, respectively. Rotational order-disorder of oxy-anions (CO_3) and displacement of cation (Ca) take place because of the impact of shock waves thereby the observed ternary switchable phase transition results paving the way for the design of new multifunctional materials.

Key-words: $CaCO_3$, Shock waves, Order –disorder phase transition, Switchable phase transition

Introduction

A few well-known materials under various physical conditions can reveal remarkable surprises of hidden facts as and when persistent observations are being carried out. Exploring

phase change behavior of materials at high-pressure and high-temperature conditions is a fascinating journey for the researchers as it consistently provides new information on the crystallographic structures and their functions in accordance with various ranges of applied pressure and temperature. In recent years, searching for new phase change materials (crystal – crystal, crystal – amorphous and amorphous – crystal) has attained a tremendous momentum due to their remarkable applications in various fields cutting across all the branches of science. These materials can give rise to outstanding performances which depend on their specific solid-state crystallographic phase that exists at a particular physical condition. Moreover, such kinds of phase transition experiments conducted on materials have significant academic as well as industrial importance due to their potential contribution for spectacular applications. Over the years, phase transition of several crystalline and non – crystalline materials have been extensively studied experimentally at static high-pressure, dynamic high-pressure, high-pressure compression and dynamic shock wave loaded conditions which have resulted in a variety of phase transitions routes that include forward and backward phase transition giving rise to crystal–crystal, amorphous–crystal and crystal–amorphous phase transitions[1-6]. Apart from the above-mentioned phase transitions, switchable phase transition has also been observed which is always considered as the special case among the phase transitions. On the one hand, reversible phase transition is quite common in static pressure compression experiments [7-12]. On the other hand, reversible crystallographic phase transition occurring at dynamic shock wave loaded conditions is quite unusual because there is no apparent report available on it in the literature, to date, at shocked conditions.

Calcium carbonate ($CaCO_3$) has been chosen for the experimental investigation because of the possible crystallographic phase transition that it might undergo at shocked conditions. Being one of the standout polymorphic minerals present on the earth, it has occupied a wide range of coverage in the literature wherein the experimental details of the obtained high-pressure polymorphic phases have been documented over the period of the past 80 years [13-15]. Hence, it could be possible via experimentation to get a deep understanding of the mechanism of polymorphic phase transitions with respect to pressure and temperature. Furthermore, there are possibly two major reasons in choosing the material for the present shock wave recovery experiment in which the first reason is that it is essential to understand the earth minerals in

terms of global carbon recycle process with respect to the existing pressure and temperature as carbonates ($CaCO_3$ and $MgCO_3$) hold a major role in the processes of global carbon recycling and climate changes [16, 17]. Secondly, it has a variety of applications in catalysis, ceramics, electronics, pigments, medicine, cosmetics, etc [18,19]. $CaCO_3$ has various crystallographic phases such as calcite ($R\bar{3}C$), aragonite (*Pmcn*), and vaterite ($P6_3/mmc$) which are the primary crystallographic phases and high-pressure distorted phases that are also available such as calcite-I, calcite-II, calcite-III, calcite-IV, calcite-V, aragonite-I, aragonite-II, post- aragonite, etc [20]. Calcite is the stable crystallographic phase at room temperature and aragonite is the high-pressure crystallographic phase, and vaterite is called the meta-stable phase with respect to calcite. Among the listed $CaCO_3$ polymorphs, calcite is the most technologically important material and a thermodynamically stable material at ambient pressure. It is abundantly available in nature on the earth's surface. Interestingly, calcite has five crystallographic phases such as Calcite-I ($R\bar{3}C$), Calcite-II ($P2_1/C$), Calcite-III ($C_2/C_m/P\text{-}1$), Calcite-IV (disorder phase), and calcite-V (disorder phase) in which calcite –IV and calcite – V are represented as high-pressure phases [20-22]. So far, several materials science and geological researchers have investigated and found crystallographic phase transitions in calcite with respect to pressure using static pressure compression and dynamic pressure compression experiments [20-22]. The first phase transition route from calcite I-II and calcite II-III phase transitions were observed at 1.5 GPa and 2.5 GPa pressure, respectively, by Bridgman in1938 [23]. Followed by his publication, many researchers have observed the similar phase transitions at more are less the same pressure ranges [20,24,25]. In addition to that, the following publications show that calcite–III b is obtained at 3.1 GPa while calcite-IV and calcite –V are found to be highly disordered structures and they represent high-pressure phases [26]. Redfern reviewed clearly the high-pressure phase transitions of $CaCO_3$ in the year 2000 [20]. It is known from the literature that many of the researchers have anticipated the phase transition route from calcite- I-II-III which could be reversible [20,23] whereas none of them could provide the experimental evidence. Interestingly, Tyburczy and Ahrens et al have demonstrated the shock wave compression phase transition from calcite II–III at 2.5 GPa and calcite III–II which has been observed during the release of shock pressure [27]. In 1994, Guillaume Fiquet et al revealed the reversible phase transition from Calcite–I to Calcite–III and Calcite–III to Calcite–I wherein the critical phase transition was observed at 4.1

GPa [28]. There is no report found, to date, on the dynamic shock wave induced phase transition for $CaCO_3$. Reversible magnetic phase transition has been obtained for $ZnFe_2O_4$ and Co_3O_4 nanoparticles such that $ZnFe_2O_4$ nanoparticles exhibit the phase transition of paramagnetic to super-paramagnetic behavior [29] while Co_3O_4 nanoparticles undergo super paramagnetic to paramagnetic phase transition with respect to the number of shocks [30]. More recently, switchable crystallographic phase transition has been observed in potassium sulfate crystals with respect to the number of shocks [31].

The present experimental analysis is to verify whether the switchable crystallographic phase transition of $CaCO_3$ by the dynamic impact of shock waves is achievable or not. Moreover, high-pressure chemistry consistently offers significant new information and numerous unexpected results of various compounds on experimentation. Hence, the investigation of the impact of shock waves on $CaCO_3$ is necessary to check whether there is a possibility to obtain additional unknown carbonate structures or not and the relative crystallographic structural stability of carbonates in a highly fluctuating environmental condition is essential as it is yet to be assessed.

Experimental section

Commercially available calcium carbonate ($CaCO_3$) (Sigma Aldrich) was used for the shock wave recovery experiment. Before the shock wave loading, the title compound was calcinated at 500° C for purification and it was sent for the fine grinding process so as to obtain fine nanopowder. Then, it was divided equally into five samples to be used for the experimental analysis. Among the five samples, one sample was kept as the control sample and the remaining four samples were sent for experimentation so that different numbers of shock wave loadings such as 50,100,150 and 200 pulses could be exposed. The required shock waves have been generated by an in-house tabletop semiautomatic shock tube which is capable of producing shocks up to Mach number 5. The shock tube has three sections such as driver, driven and diaphragm sections which are made of seamless steel. The driver and driven sections consist of long tubes of 48 cm and 180 cm, respectively and both have an inner diameter of 1.5 cm. Atmospheric air has been used as the input source for the required shock wave generation. While the atmospheric air is compressed into the driver section, at the critical pressure, the diaphragm

is ruptured and the shock wave is generated and moves along the driven section. The detailed mechanism and working methodology of the pressure driven shock tube is discussed in our previous publication [32]. For the present experiment, the shock waves of Mach number 2.2 with the pressure of 2.0 MPa and the temperature of 864 K have been used. The test samples have been placed one by one with the required interval between them in the sample holder which is typically placed 1cm away from the open end of the shock tube. Subsequently, 50,100,150 and 200 shock pulses have been loaded on the respective test samples with an interval of 5 sec between each shock pulse. For example, 50 pulses mean shock wave-exposed on a sample 50 times with Mach number 2.2. After the completion of the shock wave loading, the control and shock wave loaded samples have been analyzed by powder XRD and FTIR studies so as to understand the role of shock waves on $CaCO_3$. The schematic diagram of the semi-automated pressure-driven shock tube has been showcased in our previous publication [33].

Results and Discussion

Powder XRD results

A powder X-ray diffractometer (Bruker X-ray Diffractometer) has been utilized to evaluate the impact of shock waves on $CaCO_3$ NPs. Before discussing the shock wave induced effects on the test sample, it is quite mandatory to confirm the phase formation and their diffraction angle positions of the test sample (calcinated at 500° C) so that the corresponding XRD pattern is presented in Fig.1 along with the standard Calcite-I powder XRD pattern (ICSD: 20179). As seen in Fig.1, the XRD pattern of the test sample and the simulated XRD pattern are found to be well corroborated. But, the calcinated powder sample exhibits a slightly higher angle shift from the original positions and such kinds of shifts are highly usual in high-temperature experiments which occur due to thermal softening. The observed diffraction peaks are indexed using the standard pattern of JCPDS card no 47-1713 and the indexed diffraction peaks are (012), (104), (110), (113), (208) (018) and (116). Among the observed diffraction peaks, (104) is the strongest diffraction peak which is the characteristic peak of calcite $CaCO_3$ (trigonal -Rhombohedral structure) [34] and the calculated unit cell values are a=4.980, b=4.980, c= 16.862 Å and V= 360 $Å^3$, respectively. From the observed X-ray diffraction pattern of the control sample, it is clear that the synthesized $CaCO_3$ NPs belong to the calcite phase wherein no mixed phase is

found during the calcination process. Based on the assessment of the previous reports, the calcite phase is represented as calcite-I [28,34].

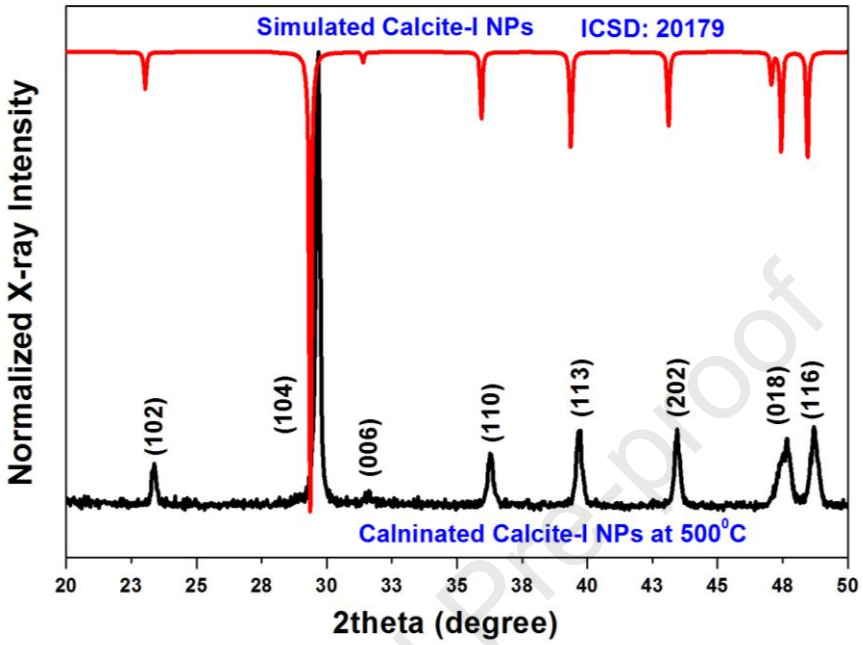

Fig.1 Powder XRD pattern of the calcinated $CaCO_3$ NPs with the simulated Calcite-I

Furthermore, special attention is paid to explore the role of shock waves on structural properties of the test samples and the corresponding XRD patterns are displayed in Fig.2. At 50 shocks, a slightly higher angle shift is observed in the diffraction peaks, especially for (104) peak. But, there is neither a new peak appearing nor the existing peaks disappearing due to the impact of shock waves. The obtained slight higher angle shift and peak broadening suggest that the calcite-I phase has transformed into Calcite –II as per the results of Merlini et al and Kaichi Suito et al [26,33]. Moreover, several high-pressure single crystal experiments have revealed the reduction of cell volume during the Calcite I-II phase transition [20,28]. In the present experiment, it is observed the higher angle shift of (104) 29.6 to 29.8 degree of crystalline peak which indicates the reduction of cell volume. The higher angle shift represents the compression of unit cells and the bond lengths of $CaCO_3$. Furthermore at 100 shocks loaded conditions, the diffraction peaks get higher angle shift and interestingly the observed diffraction peak positions

are found to be corroborated with the Calcite –III phase in accordance with the publications of Davis (1964) and Guillaume Fiquet et al (1994) [24,28].

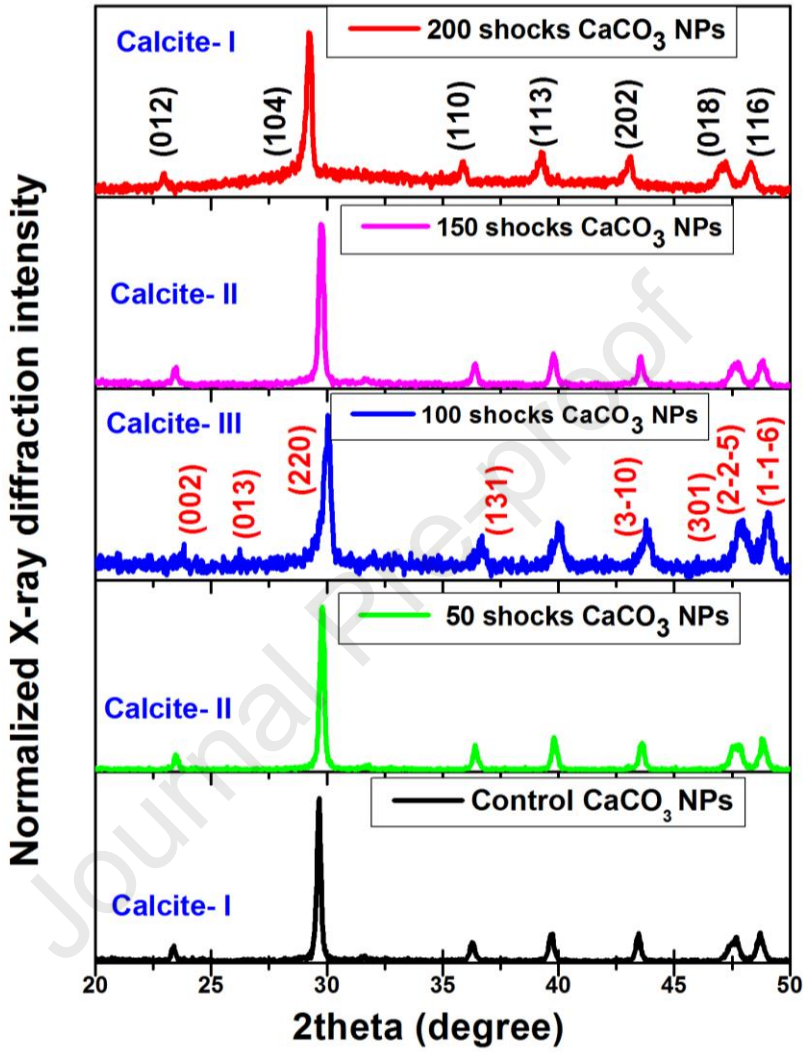

Fig.2 Powder XRD patterns of the control and shocked $CaCO_3$ NPs - Calcite phases

Calcite –III phase has the characteristic peak of (220) at 30.02 degree. Moreover, as per the above-mentioned reports, Calcite - III has a higher disorder as compared to Calcite- I and Calcite –II. According to the literature reports, it is also observed diffraction peaks of less intensity and higher broadening peaks at 100 shocks loaded a condition which is a reliable proof for the higher disorder phase than that of calcite-I and II. Hence from the observed XRD results,

it is clear that, the test sample of Calcite is phase transformed from Calcite –I to Calcite –II and Calcite –II to Calcite –III at 50 and 100 shocks loaded conditions, respectively. The observed phase transition route from Calcite –I-II-III is found to be well corroborated with the reported high-pressure calcite phase transitions [24,28,33]. Rotation of oxy-anions and displacements of cations are involved during the phase transitions and in each case, the degree of rotation and displacement is significantly varied. The detailed mechanisms of these phase transitions are to be discussed in the later sections. Furthermore, the number of shock pulses is increased to 150 and 200 shocks to get the possible understanding of the phase diagram of the calcite phase with respect to the number of shock pulses as found in pressure-temperature phase diagram of the calcite [24,28,34]. Before recording the XRD measurements of samples, it has been anticipated either to get Calcite III b phase or Calcite-IV phase at 150 and 200 shocks, respectively as obtained in the case of static high-pressure experiments [34,35].

On the other hand, fascinating results of calcite have been obtained quite unexpectedly such that 150 and 200 shocked samples have exhibited calcite –II and Calcite-I phases, respectively and the corresponding XRD patterns are presented in Fig.2. Interestingly, this happens to be the spectacular phase transition route as compared to the so far reported shock wave induced phase transitions as well as static high-pressure phase transitions of $CaCO_3$ [30,32,34,35]. For a better understanding of peak shifting and peak broadening of the characteristic crystalline peaks of (104) and (113), zoomed-in version of the respective XRD profiles are presented in Fig.3 and Fig.4 by which it is clear that the control and 200 shocked samples belong to calcite-I whereas 50, as well as 150 shocked samples, belong to Calcite-II phase while 100 shocks loaded sample is identified with calcite-III phase. As seen in Fig.3 and Fig.4, it is very clear that there is a significant difference in diffracted peak positions of (104) and (113) peaks of the control calcite-I and shock wave induced calcite-I.

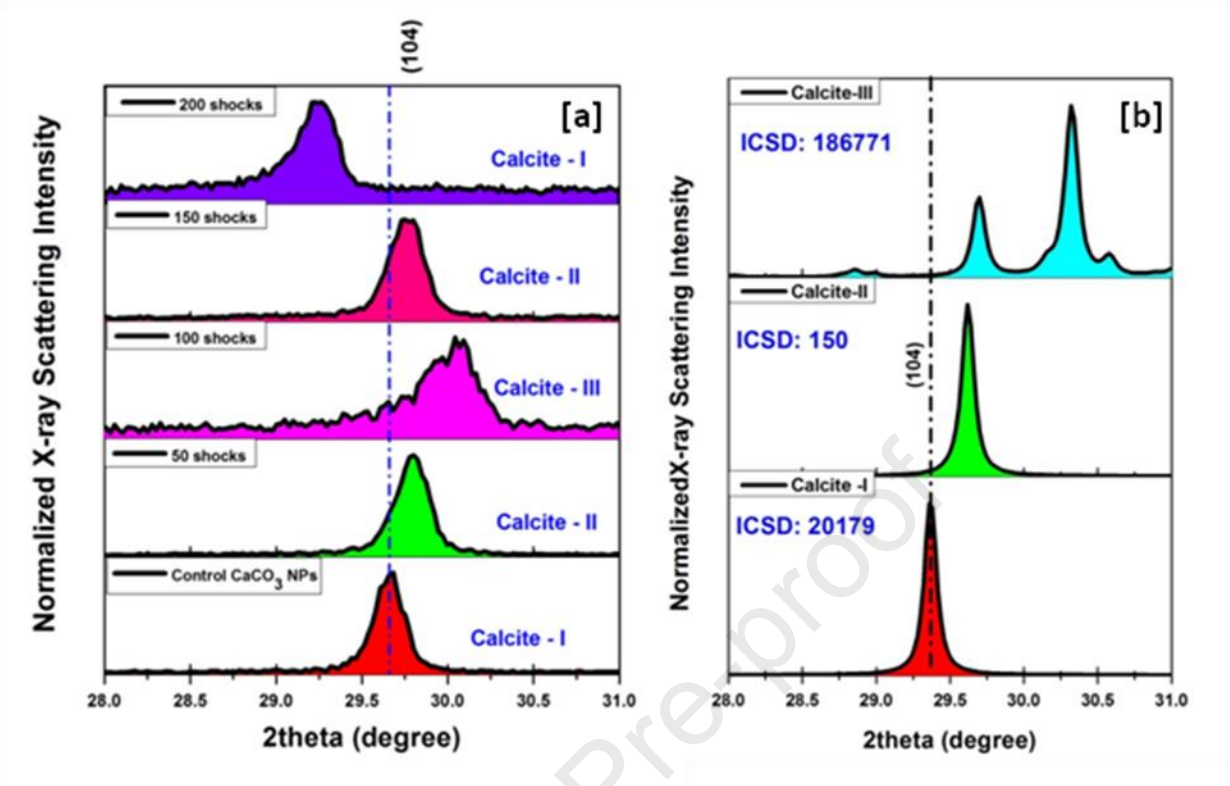

Fig.3 Zoomed-in version of crystalline peaks for the control and shocked calcite [a] (104) and [b] simulated pattern of Calcite I, II and III

During the calcination process, the test sample might have undergone the re-crystallization process and hence the (104) peak suffers a higher angle shift whereas both are found to be in the same phase. The observed XRD patterns of calcite-I, calcite-II and calcite-III are found to be well corroborated with the simulation patterns and the respective characteristic peaks of the above-mentioned calcites are presented in Fig.4. The consolidated crystallographic shock-phase profile of the calcites with respect to the number of shock pulses is presented in Fig.5.

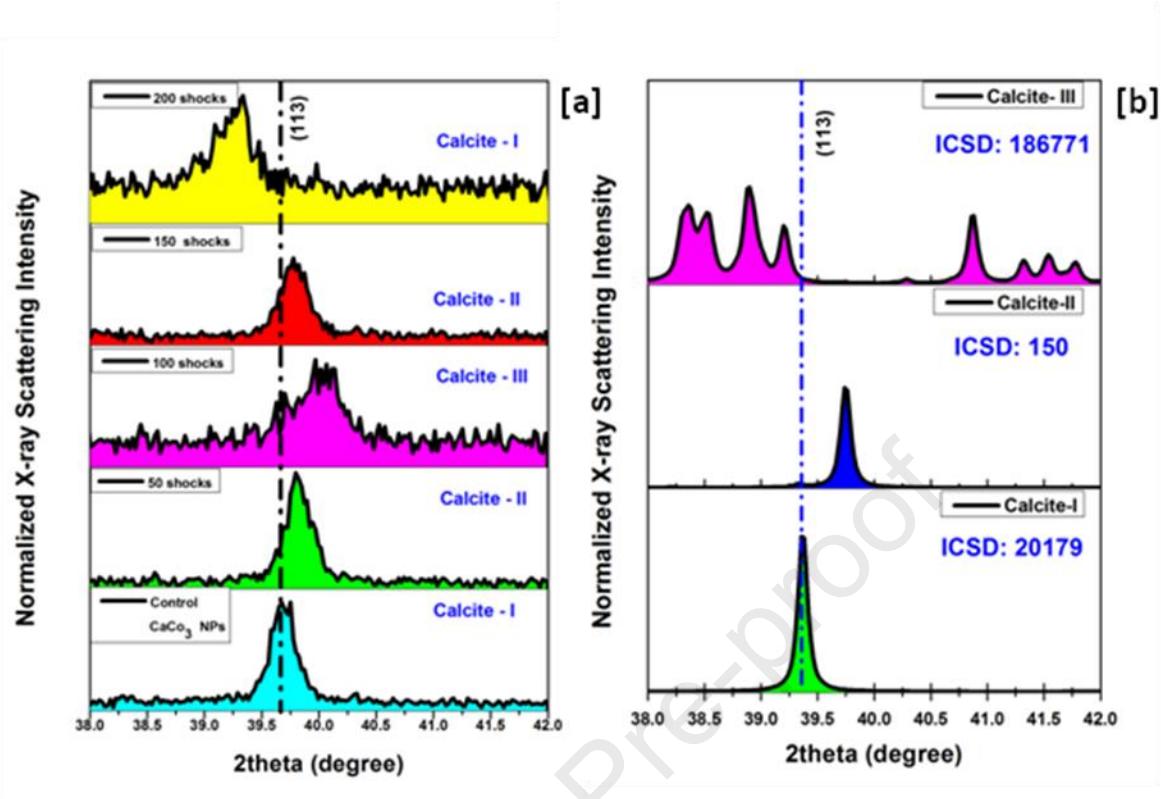

Fig.4 Zoomed-in version of the crystalline peaks of the control and shocked calcite [a] (113) and [b] simulated pattern of Calcite I, II and III

From the overall observation of XRD measurement, it is obvious that the test sample of $CaCO_3$ has undergone the switchable phase transition route of Calcite-I-II-III-II-I with respect to the control, 50,100,150 and 200 shocks loaded conditions. Note that it is probably the first observation of such kind of ternary switchable phase transition occurring between three phases of calcite. For a better understating of the ternary phase transition, the XRD patterns of simulated and 200 shocks loaded Calcite-I are presented in Fig.6 wherein both the XRD patterns are found to be well corroborated such that the ternary phase transition is confirmed. The mechanism of the phase transitions is discussed in the following sections. The grain sizes are found to be 73, 66, 59, 64, 52 nm for the control, 50,100, 150, and 200 shocked samples, respectively.

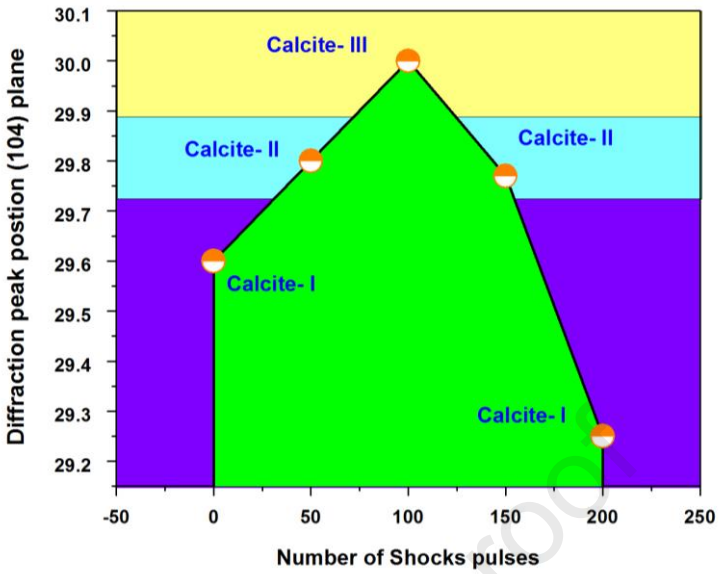

Fig.5 Shocked-phase profile of calcite with respect to the number of shock pulses

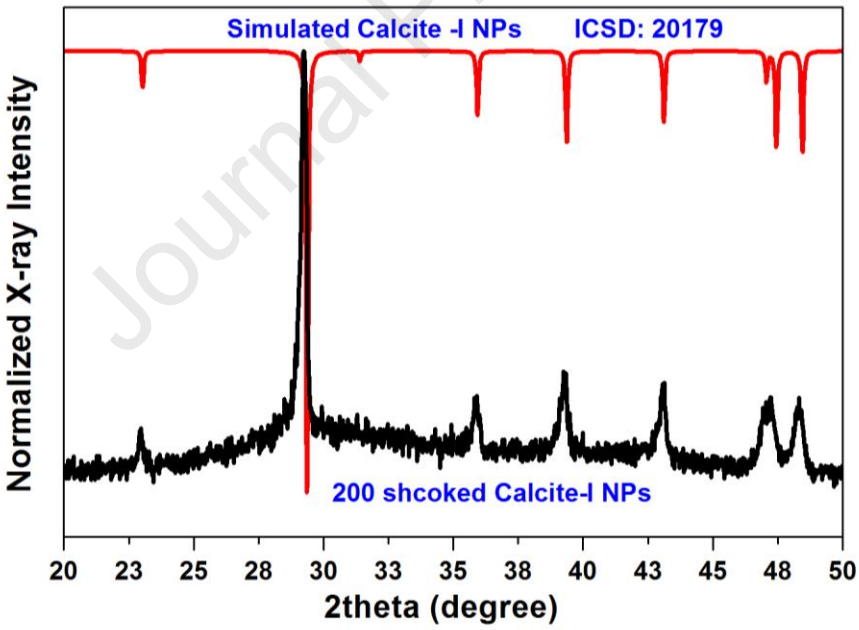

Fig.6 XRD patterns of 200 shocked and simulated Calcite-1 NPs

Calcite-I to Calcite –II phase transition

From the observed powder XRD results, it is clear that at 50 shocks, Calcite –I ($R\bar{3}C$) is phase transformed to Calcite –II ($P2_1/C$) because of the existence of strong oxy-anion rotational disorder with clockwise rotation and this kind of phase transition takes place due to the instability of the Brillouin zone at the F-point of $CaCO_3$ [20,23]. During the shock wave loaded conditions, high transient pressure is supplied to the sample so that the test material undergoes the rotational disorder effect. At a high-pressure environment, the test sample undergoes a change in its own crystallographic configuration to stay on its own chemical nature. As per the previous assessments of phase transitions of $CaCO_3$, it is proved that the carbonate groups in each c-axis layer (001) of the carbonate structures rotate in the opposite direction (rational angle is approximately 11°) with clockwise rotation in the molecular threefold axis during the Calcite-I to Calcite –II phase transition [20,23]. The space group ($R\bar{3}C$) is allowed to tilt slightly from the planer oxy-anion (CO_3) along with the clockwise rotation. In addition to that, reduction of c-axis is one of the key factors to be noticed such that better conformation of the phase transition from Calcite-I to Calcite-II could be evidenced. This conformation can be explained on the basis of the (104) peak diffraction intensity with respect to the number of shock pulses. As per the crystallographic structure of $CaCO_3$ (a=4.991, b=4.991 and c=17.062), the c-axis is 3.4 times longer than that of a and b – axes [20,23]. During the shock wave loaded condition, the c-axis undergoes a strong compression by the impact of shock waves and hence, oxy-anion (CO_3) and cation (Ca) experience rotational effect and anti-parallel displacement from the original position along with the c-axis since the planar CO_3 groups are oriented perpendicular to the c-axis. Fig.7 clearly shows the higher angle shift and peak broadening which suggest that the disordered structure has taken place due to the occurrence of rotational effect at 50 shocks. During the anti-parallel displacement of entire cation sub-lattice and oxy-anion, loss of center of symmetry has occurred so that the length of the c-axis has significantly reduced and as a result, the Calcite-II emerges at 50 shocks. The schematic diagram of the possible mechanism of shock wave induced phase transition of calcite - I- II-III is presented in Fig.7.

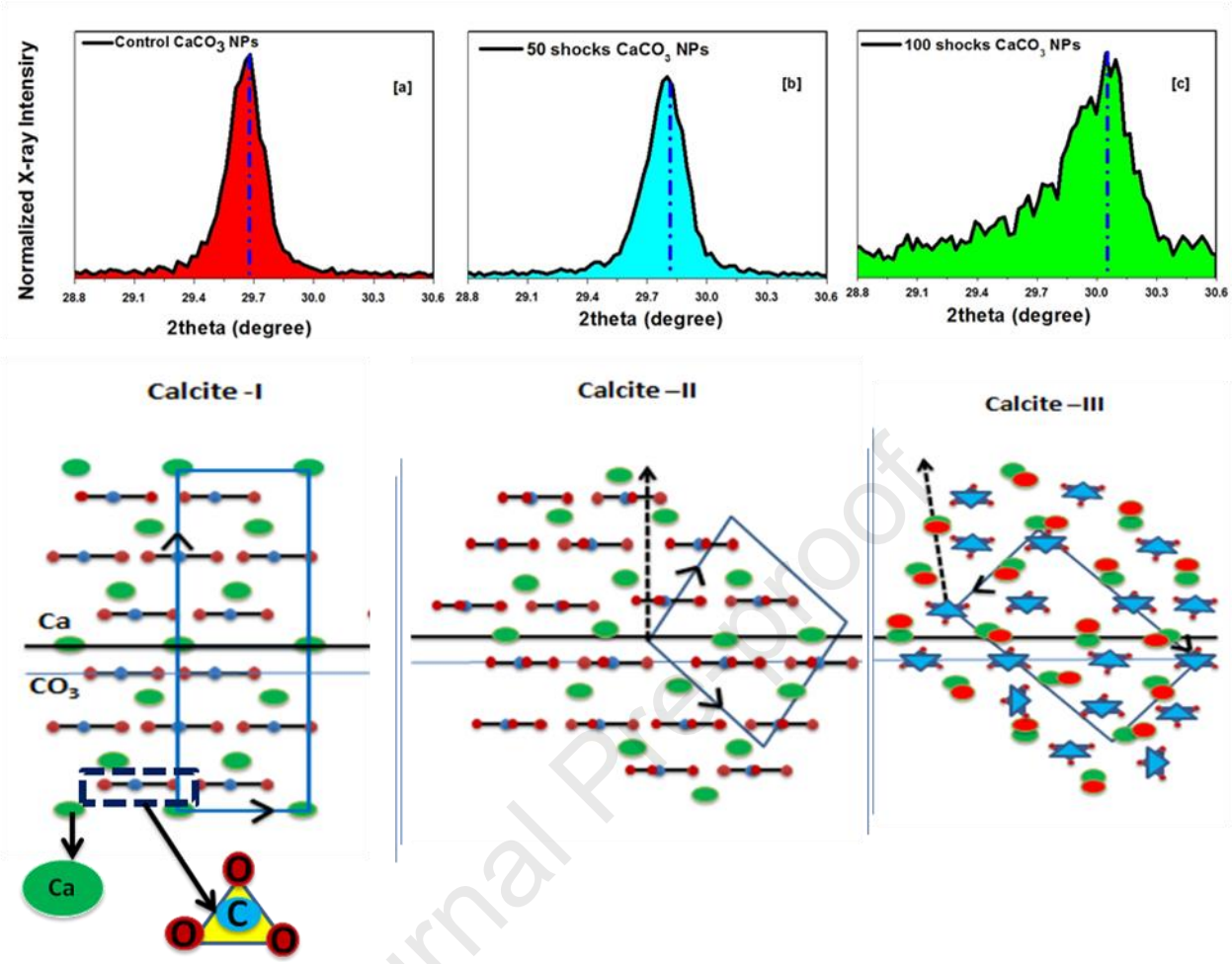

Fig.7 Possible mechanism of shock wave induced phase transition from calcite –I-II-III (a) calcite –I (b) calcite –II and (c) calcite –III (small blue ball and big red ball – displaced positions)

Calcite-II to Calcite –III phase transition

Based on the previous reports [20,23,34], the second phase transition of calcite –II to calcite –III is somewhat elusive and the above-mentioned phase transition has occurred due to the strong displacement of cations and oxy-anion rotation caused by the impact of shock waves. At this phase transition, the length of the c-axis is significantly reduced due to the strong compression of the c axis of calcite-II. Hence, there is a large volume change taking place during this phase transition due to the discontinuity of anions and cations. Moreover, the structure of calcite –III has two consecutive planes containing the c axis wherein carbonate ions are

positioned at the planes mid-way between the layers of Ca ions [36]. According to the literature, it is also observed two planes in the Calcite-III structures (Fig.7c). At 100 shocks, the test sample has experienced high transient pressure on the structures which are due to the instability of the crystal structures so that the calcite-II is phase transformed to calcite-III. At this stage, there is a strong displacement of cations and almost 90-degree rotation of oxy-anions takes place. In Fig.7c, the schematic diagram clearly shows the displacement of calcium cites (green– original and red -displaced position) and rotation of oxy-anions (CO_3). Due to the higher disorder of the crystallographic structures, calcite –III has lower symmetry and the observed XRD pattern also reveals the lower symmetry due to the lacking of strong and intense diffraction peaks. Note that, so far, there is no definite assessment found for calcite –III structure even though so many reports are available [20,23,24,28,34]. However, based on the available literature, the obtained results are found to be well corroborated with the reported XRD patterns of Davis (1964) [24], Guillaume Fiquet et al (1994) [28] and Kaichi Suito et al (2001) [33].

Reversible Phase transitions of Calcite –I-II-III-II-I

As discussed in the previous sections, the calcite phase transition takes place due to the displacement of cations and rotational order–disorder of oxy- anions. In addition to that, most of the order–disorder crystallographic phase transitions can be reversible which has been well documented in several high-pressure experiments [27,28]. The displacive atomic positions can come back to the original position and hold the ambient phase during the decompression of pressure. In the case of calcite, Guillaume Fiquet et al have demonstrated the Calcite-I-III-I switchable phase transition at 4.1 GPa. Moreover, this type of phase transition is very usual at static high-pressure compression and decompression process [28]. Remarkably in the present experiment, it is observed an array type switchable phase transition occurring between three crystallographic structures (calcite –I-II-III-II-I) at dynamic shock wave loaded conditions. To the best of our knowledge, this is the first observation made on switchable phase transition occurring between three crystallographic phases influenced by shock waves. The reason behind the switchable phase transition of calcite, at a higher number of shock wave loaded conditions, is that the oxy-anions and cations do not undergo further disorder process (calcite-IV and V) and it may be due to the dynamic physical effect of re-crystallization [31].

However, calcite-III tries to re-orient along with the crystallographic c-axis at a higher number of shocks loaded conditions. While the number of shock pulses is increased the re-orientation angle is changed so that the forward phase transition occurs with the sequence of calcite-I-II-III. Fig.8a exhibits the rotation and displacement of oxy-anion as well as cation such that Fig.8b shows the crystallographic structural shape along the view of the c-axis. Such kind of materials capable of performing an array of switchable phase transitions can be used in the environment-monitoring sensors, pressure transmitters, molecular switches, and resistive memories [37,38].

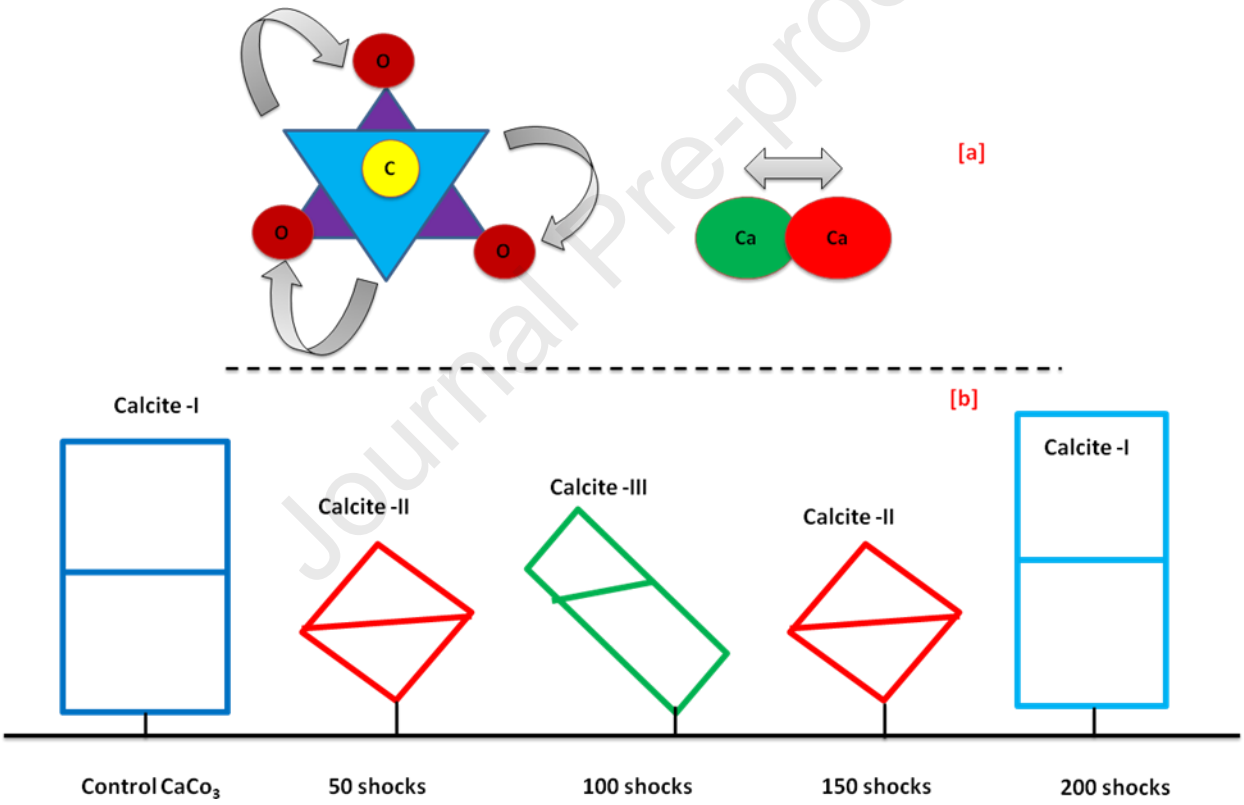

Fig.8 Schematic diagram of phase transition of calcite (a) Rotation and displacement of oxy-anion and cation (b) Calcite crystallographic structure along the view of c-axis

Fourier Transformer of Infrared (FTIR) Analysis

FTIR technique has been adopted to understand the impact of shock waves on $CaCO_3$ NPs. In the present observation, FTIR measurement has been performed over the wavenumber region of 4000-400cm^{-1} using a Perkin Elmer FTIR spectrometer and the observed FTIR spectra of the control and shocked $CaCO_3$ NPs are displayed in Fig.9. Based on the literature, carbonate molecule has four normal modes of vibration peaks i.e. In-plane bending mode ($\vartheta 4$), Out-of-plane bending mode($\vartheta 2$), Asymmetric stretching vibration carbonate ($\vartheta 1$), and Symmetric stretch of carbonate ($\vartheta 3$). As seen in Fig.9, a few FTIR bands are found as that of 708, 872, 1437 and 1801 cm^{-1} such that all the observed band positions are found to be well-matched with the characteristic bands of $CaCO_3$ [18].

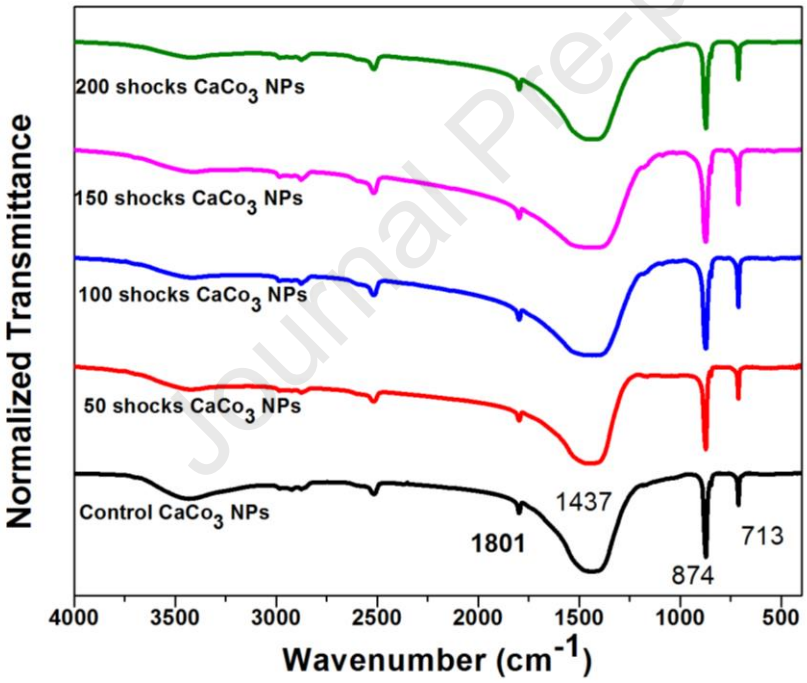

Fig.9 FTIR spectra of the control and shocked $CaCo_3$ NPs

Furthermore, among the observed FTIR bands, the bands of 708 and 872 cm^{-1} are the characteristic peaks of calcite – $CaCO_3$ NPs [18, 39]. The control and shocked samples exhibit the same number of bands and also the band positions are found to be not altered. Hence, it is

confirmed that the calcite phase is reproducible at shocked conditions. The band positions and their respective tentative assignments are presented in Table.1.

Table.1 FITR band positions and tentative assignments of $CaCO_3$ NPs

S.No	Wavenumber (cm^{-1})	Bending modes
1	708	In-plane bending mode ($\vartheta 4$)
2	872	Out-of-plane bending mode ($\vartheta 2$)
3	1437	Asymmetric stretching vibration carbonate ($\vartheta 1$)
4	1801	Symmetric stretch of carbonate ($\vartheta 3$)

From FTIR analysis, it is quite complicated to identify the difference between calcite-I, calcite-II and calcite –III phases. At shocked conditions, all the characteristics bands are reproduced and there is no peak shift, i.e. neither red shift nor blue shift observed at shocked conditions. Whereas slight changes could be observed in the intensity of the bands with respect to the number of shock waves as found in the corresponding FTIR spectra of ($\vartheta 2$) ($\vartheta 4$) bands. As seen in Fig.10, up to 100 shocks, the above-mentioned FTIR bands' intensity is slightly reduced with respect to the number of shocks and then increased at 150 and 200 shocks. It may be due to the presence of rotational disorder of oxy-anions and displacement of cations of $CaCO_3$ with the existence of disorder-order transitions and the results are known to be well corroborated with the XRD. In addition to that, ($\vartheta 4$) band intensity is continually increased at 50 and 100 shocks whereas it is reduced at 150 and 200 shocks. Opposite trending results have been observed in the case of($\vartheta 2$) band. Furthermore, the full-width half maximum (FWHM) of the control and shocked samples' 874 cm^{-1} band is measured and the corresponding FTIR spectra are presented in Fig.11a and peak fitting profiles are presented in Fig.11b. In general, for any diffraction and vibration spectra, the values of lower FWHM suggest a good structural order and a higher grain size [40,41]. As seen in Fig.11, the values of FWHM are found to be 16, 18, 26, 24, and 19 cm^{-1} for the control, 50, 100,150 and 200 shocks, respectively. The observed values of FWHM for $CaCO_3$ is found to be continually increasing up to 100 shocks whereas they appear to

have reduced at 150 and 200 shocks and the results are known to be well corroborated with the values obtained in the calculation of the XRD grain size.

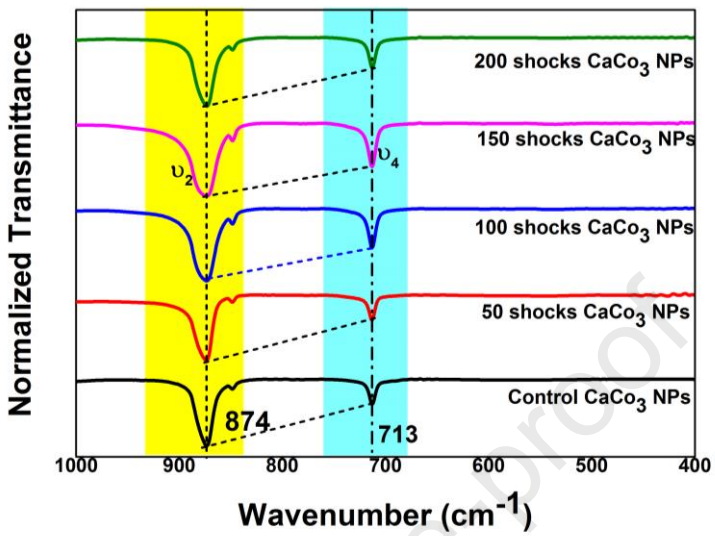

Fig.10 FTIR spectra of the selected region (1000-400 cm^{-1}) of the control and shocked samples

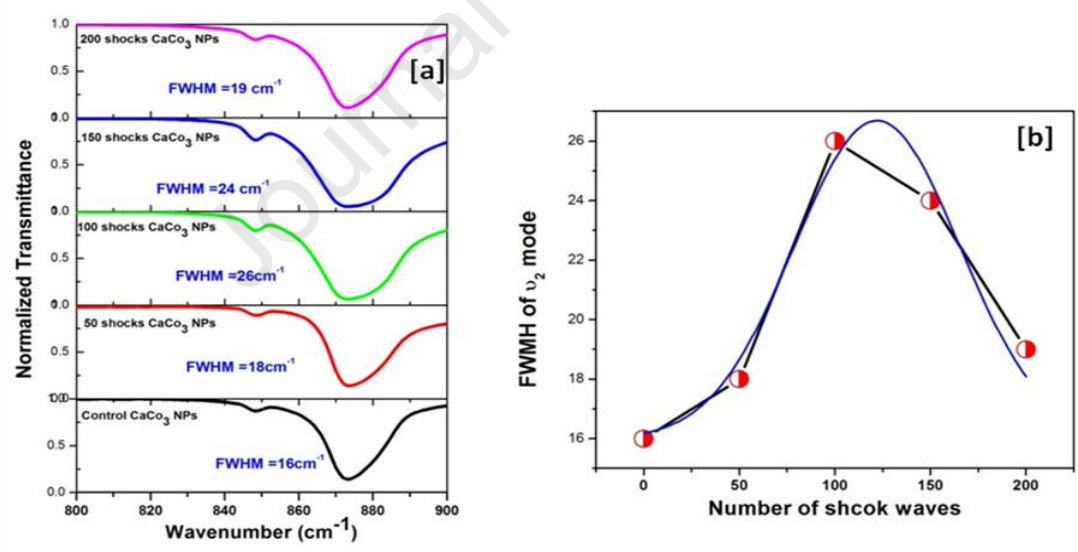

Fig.11 FWHM values of out-of-plane bending mode($\vartheta 2$) for the control and shocked $CaCO_3$

Conclusion

In summing-up of the experimental findings, switchable crystallographic phase transition between calcite-I, calcite-II and calcite –III has been observed for $CaCO_3$ NPs at the exposure of shock waves of Mach number 2.2. It is quite interesting that such kind of observation has not been reported till this point in time which is an array of switchable crystallographic phase transitions of calcite with the sequence of I-II-III-II-I. On increasing the number of shock waves, the observed powder XRD patterns of the samples clearly exhibit the array of switchable phase transitions occurring between low-pressure calcite phases. FTIR band assignments and band patterns provide the possible supporting evidence for the observed switchable phase transitions between low-pressure calcite phases. During the shock wave loaded conditions, rotational disorder-order of oxy-anions (CO_3) and translation displacement of cation (Ca) take place and these changes induce the switchable crystallographic phase transition between calcite-I-II-III. Such kind of array of switchable phase transitions offer a new possibility for the making of devices such as environment-monitoring sensors, pressure transmitters, molecular switches, and resistive memories along with the scope to design new multifunctional materials so that the calcite NPs are strongly suggested to be a potential candidate for the above-mentioned applications.

Compliance with ethical standards

None

Conflict of interest

The authors declare that they have no conflict of interest**.**

Acknowledgement

The authors thank Department of Science and Technology (DST), India for DST-FIST progarmme (SR/FST/College-2017/130 (c)). The project was supported by Researchers Supporting Project number (RSP-2021/231), King Saud University, Riyadh, Saudi Arabia.

References

[1] Lijun Zhang, Yanchao Wang, Jian Lv and Yanming Ma, Materials discovery at high pressures. Nat.Rev.Mater **2**, 17005 (2017) DOI: https://doi.org/10.1038/natrevmats.2017.5

[2] Linfei Yang, Jianjun Jiang, Lidong Dai, Haiying Hu, Meiling Hong, Xinyu Zhang, Heping Li and Pengfei Liu. High-pressure structural phase transition and metallization in Ga_2S_3 under non-hydrostatic and hydrostatic conditions up to 36.4 GPa. J. Mater. Chem. C, 9, 2912 (2021) DOI: https://doi.org/10.1039/d0tc06004f

[3] Zhi Su, William L. Shaw, Yu-Run Miao, Sizhu You, Dana D. Dlott, and Kenneth S. Suslick, Shock Wave Chemistry in a Metal−Organic Framework. J. Am. Chem. Soc. **139** 4619–4622 (2017) DOI: https://doi.org/10.1021/jacs.6b12956

[4] Lidong Daia, Yukai Zhuangab, Heping Lia, Lei Wua, Haiying Hua, Kaixiang Liuab, Linfei Yangab and Chang Pu; Pressure-induced irreversible amorphization and metallization with a structural phase transition in arsenic telluride. J. Mater. Chem. C, 5, 12157-12162 (2017) DOI: https://doi.org/10.1039/x0xx00000x

[5] Lidong Dai, Kaixiang Liu, Heping Li, Lei Wu, Haiying Hu, Yukai Zhuang, Linfei Yang, Chang Pu, and Pengfei Liu. Pressure-induced irreversible metallization accompanying the phase transitions in Sb_2S_3. Phys. Rev. B 97, 024103 (2018) DOI: https://doi.org/10.1103/PhysRevB.97.024103

[6] Lei Kang, Kai Wang, Shourui Li, Jing Liu, Ke Yang, Bingbing Liu, and Bo Zou, Pressure-Induced Phase Transition in Hydrogen-Bonded Supramolecular Structure: Ammonium Formate. J. Phys. Chem. C. **118**, 8521 (2014) DOI: https://doi.org/10.1021/jp412112g

[7] Wojciech Wełnic and Matthias Wuttig, Reversible switching in phase-change materials. *Mater.Today*. **11**, 20-27 (2008) DOI: https://doi.org/10.1016/S1369-7021(08)70118-4

[8] Wen-Wen Fan, Yi Cheng, Prof. Li-Yan Zheng, Dr. Qiu-E. Cao; Reversible Phase Transition of Porous Coordination Polymers. Chem. Eur. J. **13**, 2766-2779 (2020) DOI: https://doi.org/10.1002/chem.201903985

[9] M. Andrzejewski, N. Casati and A. Katrusiak, Reversible Pressure Preamorphization of a Piezochromic MetalOrganic Framework. Dalton Trans. **46**, 14795-14803 (2017) DOI: https://doi.org/10.1039/C7DT02511D

Journal Pre-proof

[10] Thomas D. Bennett, Petra Simoncic, Stephen A. Moggach, Fabia Gozzo, Piero Macchi, David A. Keen, Jin-Chong Tan and Anthony K. Cheetham; Reversible pressure-induced amorphization of a zeolitic imidazolate framework (ZIF-4). Chem. Commun. **47,** 7983–7985 (2011) DOI: https://doi.org/10.1039/C1CC11985K

[11] Kohji Tashiro, Jue Cheng, and Miyuki Ike; Stress-Induced Reversible Phase Transition of Poly(tetramethylene naphthalate). Macromolecules, **36**, 359-367 (2003) DOI: https://doi.org/10.1021/ma020917d

[12] Kai Wang, Jing Liu, Ke Yang, Bingbing Liu, and Bo Zou; High-Pressure-Induced Reversible Phase Transition in Sulfamide. J. Phys. Chem. C. **118**, 18640−18645 (2014**)** DOI: https://doi.org/10.1021/jp504641z

[13] Peter Németh, Enrico Mugnaioli, Mauro Gemmi, György Czuppon, Attila Demény and Christoph Spotl; A nanocrystalline monoclinic $CaCO_3$ precursor of metastable aragonite. Sci. Adv **4**, 6178 – 6185 (2018) DOI: https://doi.org/10.1126/sciadv.aau6178

[14] Michael S. Bodnarchuk, David M. Heyes, Angela Breakspear, Samir Chahine, Simon Edwards, and Daniele Dini; Response of Calcium Carbonate Nanoparticles in Hydrophobic Solvent to Pressure, Temperature and Water. J. Phys. Chem. C, **119** 16879–16888 (2015) DOI: https://doi.org/10.1021/acs.jpcc.5b00364

[15] Nobuo Ishizawa, Hayato Setoguchi and Kazumichi Yanagisawa; Structural evolution of calcite at high temperatures: Phase V unveiled. Sci.Rep. **3,** 2832 (2013) DOI: https://doi.org/10.1038/srep02832

[16] Xi Yao, Congwei Xie, Xiao Dong, Artem R. Oganov, and Qingfeng Zeng; Novel high-pressure calcium carbonates. Phys.Rev. B. **98**, 014108 (2018) DOI: https://doi.org/10.1103/PhysRevB.98.014108

[17] Pavel N. Gavryushkin, Naira S. Martirosyan, Talgat M. Inerbaev, Zakhar I. Popov, Sergey V. Rashchenko, Anna Yu. Likhacheva, Sergey S. Lobanov, Alexander F. Goncharov, Vitali B. Prakapenka, and Konstantin D. Litasov, Aragonite-II and $CaCO_3$-VII: New High-Pressure, High-Temperature Polymorphs of $CaCO_3$. Cryst. Growth Des. **17,** 6291−6296. (2017) DOI: https://doi.org/10.1021/acs.cgd.7b00977

[18] Sanaz Abdolmohammadi, Samira Siyamak, Nor Azowa Ibrahim, Wan Md Zin Wan Yunus, Mohamad Zaki Ab Rahman, Susan Azizi, and Asma Fatehi ; Enhancement of

Mechanical and Thermal Properties of Polycaprolactone/Chitosan Blend by Calcium Carbonate Nanoparticles. Int. J. Mol. Sci. **13,** 4508-4522 (2012) DOI: https://doi.org/10.3390/ijms13044508

[19] Daria B.Trushina, Tatiana V.Bukreeva, Mikhail V.Kovalchuk, Maria N.Antipina; $CaCO_3$ vaterite microparticles for biomedical and personal care applications. Mater. Sci.Eng C. **45**, 644–658 (2014) DOI: https://doi.org/10.1016/j.msec.2014.04.050

[20] Simon A. T. Redfern; Structural Variations in Carbonates. Rev Mineral Geochem. **41**, 289–308 (2000) DOI: https://doi.org/10.2138/rmg.2000.41.10

[21] Sergey S. Lobanov, Xiao Dong, Naira S. Martirosyan, Artem I. Samtsevich, Vladan Stevanovic, Pavel N. Gavryushkin, Konstantin D. Litasov, Eran Greenberg, Vitali B. Prakapenka, Artem R. Oganov, and Alexander F. Goncharov; Raman spectroscopy and X-ray diffraction of sp3-$CaCO_3$ at lower mantle pressures. Phys. Rev. B, **96,** 104101 (2017) DOI: https://doi.org/10.1103/PhysRevB.96.104101

[22] Kenji Hagiya, Masanori Matsui, Yuhei KImura, Yuichi Akahama. The crystal data and stability of calcite III at high pressures based on single－crystal X－ray experiments. J.Miner.Petrol Sci**, 100**, 31－36 (2005) DOI: https://doi.org/10.2465/jmps.100.31

[23] P.W.Bridgman; The high pressure behavior of miscellaneous minerals. Am. J. Sci. **237**, 7－18 (1939) DOI: https://doi.org/10.2475/ajs.237.1.7

[24] B. L.Davis; X-ray Diffraction Data on Two High-Pressure Phases of Calcium Carbonate. Science, **145**, 489-491 (1964) DOI: https://doi.org/10.1126/science.145.3631.489

[25] R. S.Joseph.; and J.A.Thomas, The crystal structure of calciteIII. Geophys.Res.Lett **24,** 1595-1598 (1997) DOI: https://doi.org/10.1029/97GL01603

[26] M.Merlini, W.A. Crichton, J.Chantel, J.Guignard, and S.Poli; Evidence of interspersed co-existing CaCO3-III and CaCO3-IIIb structures in polycrystalline $CaCO_3$ at high pressure. Mineral.Mag. **78**, 225–233 (2014) DOI: https://doi.org/10.1180/minmag.2014.078.2.01

[27] A.T.James, and J.A.Thomas; Dynamic compression and volatile release of carbonates; J. Geophys. Res. **91**, 4730-4744 (1986) DOI: https://doi.org/10.1029/JB091iB05p04730

[28] F.Guillaume, G.Francois, I.Jean-Paul, High-pressure X-ray diffraction study of carbonates: $MgCO_3$, $CaMg(CO_3)_2$, and $CaCO_3$. Amer Miner, **79**, 15–23 (1994)

[29] V.Mowlika, A.Sivakumar, S.A.Martin Britto Dhas, C.S.Naveen, A.R.Phani, R.Robert, Shock wave-induced switchable magnetic phase transition behaviour of $ZnFe_2O_4$ ferrite Nanoparticles. J.Nanostcture. Chem. **10**, 203–209 (2020)
DOI: https://doi.org/10.1007/s40097-020-00342-0

[30] A.Sivakumar, S.Soundarya, S.Sahaya Jude Dhas, K.Kamala Bharathi and S.A. Martin Britto Dhas; Shock Wave Driven Solid State Phase Transformation of Co_3O_4 to CoO Nanoparticles. J.Phys.Chem.C. **124**, 10755–10763 (2020)
DOI: https://doi.org/10.1021/acs.jpcc.0c02146

[31] A.Sivakumar, S.Reena Devi, S.Sahaya Jude Dhas, R.Mohan Kumar, K. Kamala Bharathi, and S.A.Martin Britto Dhas, Switchable Phase Transformation (Orthorhombic - Hexagonal) of Potassium Sulfate Single Crystal at Ambient Temperature by Shock Waves. Cryst.Growth.Des. **20** 7111–7119, (2020)
DOI: https://doi.org/10.1021/acs.cgd.0c00214

[32] A.Sivakumar, S.Balachandar, S.A.Martin Britto Dhas; Measurement of "Shock Wave Parameters" in a Novel Table-Top Shock Tube Using Microphones. Hum.Factors.Mech. Eng.Def. Saf. **4**, 1-6, (2020) DOI: https://doi.org/10.1007/s41314-019-0033-5

[33] S.Kalaiarasi, A. Sivakumar, S.A.Martin Britto Dhas, M.Jose, Shock wave induced anatase to rutile TiO_2 phase transition using pressure driven shock tube. Mater. Lett. **219**, 72–75 (2018) DOI: https://doi.org/10.1016/j.matlet.2018.02.064

[34] Kaichi Suito, Junpei Namba, Takashi Horikawa, Yozo Taniguchi, Noriko Sakurai, Michihiro Kobayashi, Akifumi Onodera, Osamu Shimomura and Takumi Kikegawa; Phase relations of $CaCO_3$ at high pressure and high temperature. Amer Miner, 86, 997–1002 (2001) DOI: https://doi.org/10.2138/am-2001-8-906

[35] Jin Liu, Razvan Caracas, Dawei Fan, Ema Bobocioiu, Dongzhou Zhang and Wendy L. Mao , High- pressure compressibility and vibrational properties of (Ca,Mn)CO3. Amer Miner. 101, 2723–2730 (2016) DOI: https://doi.org/10.2138/am-2016-5742

[36] T. Pippinger, R. Miletich, M. Merlini, P. Lotti, P. Schouwink, T. Yagi, W. A. Crichton and M. Hanfland; Puzzling calcite‐III dimorphism: crystallography, high‐pressure

behavior, and pathway of single‐crystal transitions. Phys Chem Miner.**,** 42, 29–43 (2015) DOI: https://doi.org/10.1007/s00269-014-0696-7

[37] Xueyin Yuan, Xin Xiong, Guoliang Zhang, Robert A. Mayanovic; Application of calcite, Mg-calcite, and dolomite as Raman pressure sensors for high-pressure, high-temperature studies. J.Raman Spectrosc. 511248-1259 (2020) DOI: https://doi.org/10.1002/jrs.5893

[38] Robert Haaring, Naveen Kumar, Duco Bosma, Lukasz Poltorak, and Ernst J. R. Sudholter Electrochemically Assisted Deposition of Calcite for Application in Surfactant Adsorption Studies. Energy Fuels. 33, 805−813 (2019) DOI: https://doi.org/10.1021/acs.energyfuels.8b03572

[39] Johannes Ihli, Wai Ching Wong, Elizabeth H. Noel, Yi-Yeoun Kim, Alexander N. Kulak, Hugo K. Christenson, Melinda J. Duer & Fiona C. Meldrum; Dehydration and crystallization of amorphous calcium carbonate in solution and in air. Nat.Comm. 5, 3169 (2014) DOI: https://doi.org/10.1038/ncomms4169

[40] M.Chmielov and Z.Weiss, Determination of structural disorder degree using an XRD profile fitting procedure. Application to Czech kaolins. Appl. Clay Sci. 22, 65–74 (2002) DOI: https://doi.org/10.1016/S0169-1317(02)00114-X

[41] C. Koike, J. Matsuno, and H. Chihara; Variations in the Infrared Spectra of Wustite with Defects and Disorder. Ap.J. 845, 15 (2017) DOI: https://doi.org/10.3847/1538-4357/aa7deb

Journal Pre-proof

Journal Pre-proof

Compliance with ethical standards

None

Conflict of interest

The authors declare that they have no conflict of interest**.**

Journal Pre-proof